Low Temperature Physics/Fizika Nizkikh Temperatur, 2020, v. 46, No. 8, pp. 914–919

Theoretical models of diffusion-attenuated magnetic resonance signal in biological tissues

Alexander L. Sukstanskii and Dmitriy A. Yablonskiy

Mallinckrodt Institute of Radiology, Washington University School of Medicine, St. Louis, USA
E-mail: asukstansky@wustl.edu; YablonskiyD@wustl.edu

Received March 5, 2020, published online June 22, 2020

Diffusion Magnetic Resonance Imaging (MRI) plays a very important role in studying biological tissue cellular structure and functioning both in health and disease. Proper interpretation of experimental data requires the development of theoretical models that connect the diffusion MRI signal to salient features of tissue microstructure at the cellular level. In this short review, we present some theoretical approaches to describing diffusion-attenuated magnetic resonance signals. These range from the models based on statistical properties of water molecules diffusing in the tissue-cellular environment, to models allowing exact analytical calculation of the magnetic resonance signal in a specific single-compartment environment. Such theoretical analysis gives important insights into mechanisms contributing to the formation of diffusion magnetic resonance signal and its connection to biological tissue cellular structure.

Keywords: magnetic resonance, Gaussian phase approximation, multiple propagator approach.

Introduction

Diffusion Magnetic Resonance Imaging (MRI) is a technique that is capable of providing *in vivo* images with a contrast uniquely sensitive to molecular displacement motion at cellular and sub-cellular length scales. Despite a rather long history and substantial progress in both clinical and research applications, the biophysical mechanisms underlying this contrast are not always understood. This is not surprising because biological tissues have very complicated composition and geometrical architecture — factors that influence diffusion-weighted MRI signal in multiple ways. For example, even a very small imaging voxel in the central nervous system (CNS) will always have a very complicated content due to the presence of myriads of cells with different sizes, intracellular milieu, membrane properties, etc.

The average diffusion coefficient for water in the CNS is about 1 mm^2/ms and the typical magnetic resonance (MR) diffusion experiment employs a diffusion time Δ of 20–80 ms. Thus, the average water molecule probes a length scale on the order of 5 to 20 μm, making diffusion MR sensitive to a wide range of tissue microstructural properties. The ultimate goal of MR diffusion theory is to quantitatively relate these microstructural and physiological properties to the diffusion-weighted MR signal. Due to the above mentioned highly complex tissue structure, these theories can never be perfect and can never ideally fit experimental data. However, as long as they reflect tissue properties of interest, they serve the purpose. The MR relevant range of length scales for restrictions and hindrances to water diffusion should be reflected in any model of MR diffusion data from biological systems.

In what follows, we consider (i) the case of unrestricted diffusion, in which the problem can be solved analytically; (ii) diffusion restricted by the boundary of simple geometry, for which the eigenfunction of the diffusion equation is available; in this case, the signal can be calculated in the framework of the multiple propagator approach; (iii) diffusion restricted by boundaries of arbitrary geometry in the short-time approximation.

General approach

Most MR methods for measuring molecular displacement rely on a Stejskal–Tanner pulsed gradient experiment [1] depicted in Fig. 1. This pulse sequence consists of an initial 90° radio-frequency (RF) excitation pulse followed by bipolar diffusion-sensitizing magnetic field gradient

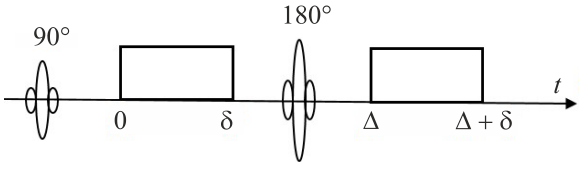

Fig. 1. The Stejskal–Tanner pulsed gradient pulse sequence. The signal is measured either after the first gradient lobe (free induction decay, FID) or after the second gradient lobe (spin echo, SE).

pulses separated by a 180° refocusing RF pulse. Characteristic parameters of the waveform are the gradient amplitude G, the diffusion time Δ, and the pulse width δ.

In a general case, the signal produced by a system of a large number of precessing spins at time t after the first RF pulse is

$$S(t) = S_0 \cdot s(t), \qquad s(t) = \left\langle \exp\left[-i\,\varphi(t)\right]\right\rangle, \tag{1}$$

where the factor S_0 describes the signal in the absence of diffusion-sensitizing gradients and accounts for the transverse T_2 relaxation, $\varphi(t)$ is the phase accumulated by a single spin by time t, and $\langle\ldots\rangle$ means averaging over all possible initial positions and trajectories. In an inhomogeneous magnetic field, $\mathbf{H} = \mathbf{H}(\mathbf{r}, t)$, the phase $\varphi(t)$ of the spin moving along a given trajectory $\mathbf{r} = \mathbf{r}(t)$ can be written as

$$\varphi(t) = \int_0^t dt'\,\omega\left(\mathbf{r}(t'), t'\right), \tag{2}$$

where the local Larmor frequency $\omega = \gamma H$, γ is the gyromagnetic ratio. The phase in Eq. (2) depends on all the points of the trajectory. Diffusion of molecules (e.g., water) is described by a diffusion propagator $P(\mathbf{r}, \mathbf{r}_0, t)$ satisfying the diffusion equation:

$$\partial P / \partial t = D \cdot \nabla^2 P \tag{3}$$

(D is the diffusion coefficient) with the initial condition $P(\mathbf{r}, \mathbf{r}_0, 0) = \delta(\mathbf{r} - \mathbf{r}_0)$, and with specific boundary conditions.

Another approach for calculating the MR signal is based on the Bloch–Torrey equation for the magnetization distribution $m(\mathbf{r}, t)$ — a circular component of transverse (with respect to the external field $\mathbf{H}_0$ magnetization distribution ($m = m_x + i m_y$) at time t after the excitation RF pulse [2]:

$$s(t) = \int d\mathbf{r}\, m(\mathbf{r}, t),$$
$$\frac{\partial m(\mathbf{r}, t)}{\partial t} = \hat{L}\, m(\mathbf{r}, t), \quad \hat{L} = D\nabla^2 + i\gamma h_z(\mathbf{r}, t), \quad m(\mathbf{r}, 0) = \rho_0(\mathbf{r}), \tag{4}$$

where $h_z(\mathbf{r}, t) = H_0 + \mathbf{G}(t) \cdot \mathbf{r}$. Importantly, the operator $\hat{L}$ is non-Hermitian, and an analytical solution of Eq. (4) for an arbitrary $\mathbf{G}(t)$ in a closed analytical form is available only in the case of unrestricted diffusion and in the one-dimensional case [3].

Let us consider first the case of unrestricted (free) diffusion. In a homogeneous unbounded media (e.g., water) thermal molecular motion is random, and the diffusion propagator $P(\mathbf{r}, \mathbf{r}_0, t)$ is Gaussian, and the SE signal is a simple mono-exponential function [1]:

$$S = S_0 \exp\left(-b\, D_0\right). \tag{5}$$

Here D_0 is the free diffusion coefficient for water molecules or other MR active species under consideration; b is the so-called b-value. For an arbitrary gradient waveform $\mathrm{G}(t)$ applied during a total time T [4]:

$$b = \gamma^2 \int_0^T dt \left[\int_0^t dt'\, \mathbf{G}(t')\right]^2. \tag{6}$$

For Stejskal–Tanner pulse sequence, Eq. (6) reduces to $b = (\gamma G \delta)^2 (\Delta - \delta/3)$.

As demonstrated in [5], in the case of free diffusion the phase distribution function is also Gaussian. Hence, only first two terms in the cumulant expansion of $s(t)$ in Eq. (1) differs from 0, and

$$s(t) = \exp\left[\left\langle -\varphi^2(t)/2 \right\rangle\right] \tag{7}$$

(without loss of generality, we consider $\langle\varphi\rangle = 0$). Averaging $\varphi^2(t)$ rather than the exponent $\exp(-i\,\varphi(t))$ is a substantially less challenging problem because $<\varphi^2(t)>$ can be written in a closed form:

$$\left\langle \varphi^2(t) \right\rangle = \frac{2\gamma^2}{V} \int_0^t d\tau_1 \int_0^{\tau_1} d\tau_2 \int_V d\mathbf{r}_1 \times$$
$$\times \int_V d\mathbf{r}_2 \left(\mathbf{G}(\tau_1)\cdot\mathbf{r}_1\right)\left(\mathbf{G}(\tau_2)\cdot\mathbf{r}_2\right) P(\mathbf{r}_1, \mathbf{r}_2, \tau_1 - \tau_2). \tag{8}$$

In the case of unrestricted diffusion, when the propagator is Gaussian, the integrals in Eq. (8) can be readily calculated [5] leading to the same signal as in Eq. (5).

If diffusion is restricted by some barriers or if the field gradients are non-uniform (as in the case of susceptibility-induced field inhomogeneities), the phase distribution function is, in general, not Gaussian. However, in some cases, it can be well approximated by a Gaussian function — the so-called Gaussian phase approximation (GPA). The quantity $\langle\varphi^2(t)\rangle$ and, consequently, the signal can be readily calculated in systems for which the diffusion propagator $P(\mathbf{r}_1, \mathbf{r}_2, t)$ is available. Some important examples of these calculations can be found in [6].

In the GPA both $\langle\varphi^2(t)\rangle$ in Eq. (8) and the b-value in Eq. (6) are proportional to the diffusion gradient amplitude squared, the diffusion attenuated MR signal can be presented in the form similar to Eq. (5):

$$S = S_0 \exp\left(-b \cdot \tilde{D}\right), \tag{9}$$

where $\tilde{D}$ is the so-called apparent diffusion coefficient (ADC). Obviously, for free diffusion $\tilde{D} = D_0$. In general case, $\tilde{D}$ depends on the "timing" parameters of the gradient waveform and, of course, on the structure and properties of the environment in which spins diffuse. However, in the framework of the GPA, $\tilde{D}$ does not depend on the strength of diffusion gradients (for fixed "timing" parameters of the gradient waveform).

The dependence $-\ln S \sim G^2$ is a "hallmark" of the GPA. The adequateness of this approximation has been discussed by many authors [6–10]. First, the GPA is valid at short diffusion times, when phase accumulated by diffusing spins is small, $\varphi << 1$. Second, it can be valid at sufficiently long diffusion times (this condition is necessary but not sufficient!), when all diffusing spins have encountered boundaries many times, their trajectories become statistically identical, and the central limit theorem can be applied. Obviously, this is not always true. For instance, in the case of narrow pulses, the diffusion attenuated MR signal from a single restricted compound demonstrates a quasi-periodic dependence on G (a so-called "diffusion diffraction" effect [7]). A detailed quantitative comparison of the Gaussian phase approximation with exact results for some models of restricted diffusion in the presence of a constant field gradient was given in [10] for a broad range of system parameters.

Multiple propagator approach

A rather powerful approach for the calculation of the MR signal in the presence of external magnetic field gradients has been developed in [11,12] in conjunction with studies of restricted diffusion. This approach is based on dividing the gradient pulse into successive short time intervals and then using a propagator for each stage of the evolution — the so-called "multiple propagator approach" (MPA). In [10] the MPA was reformulated in such a way to obtain not only the net signal $S(t)$ but the signal spatial density (magnetization distribution $m(\mathbf{r}, t)$) as well, i.e., to solve Eq. (4).

The MPA can be used when the diffusion propagator, i.e., the Green's function of the diffusion equation with the boundary conditions specified by the system's geometry, is known. In this case, the propagator $P(\mathbf{r},\mathbf{r}',t)$ allows the standard expansion in terms of the orthogonal set of (normalized) eigenfunctions $\{u_k(\mathbf{r}), k = 0, 1, ...\}$ of the Sturm–Liouville problem:

$$P(\mathbf{r},\mathbf{r}',t) = \frac{1}{V}\sum_{k=0}^{\infty} u_k(\mathbf{r})u_k^*(\mathbf{r}')\exp\left(-\lambda_k t\right), \qquad (10)$$

where λ_k are the corresponding eigenvalues. Dividing the spin's trajectory into N small intervals Δt, $t = N{\cdot}\Delta t$, and using Eq. (10) at each time intervals, for an arbitrary gradient waveform $\mathbf{G}(t)$ the net signal and the magnetization distribution can be obtained in a matrix product form. For the FID signal ($\mathbf{G} = \text{const}$),

$$m(\mathbf{r},t) = \boldsymbol{\varphi}\left(\mathbf{r}, \mathbf{q}/2\right)\cdot\hat{\boldsymbol{\Lambda}}(\Delta t)\cdot\left[\hat{\mathbf{U}}(\mathbf{q})\cdot\hat{\boldsymbol{\Lambda}}(\Delta t)\right]^{N-1}\cdot\mathbf{F}^{\dagger}\left(-\mathbf{q}/2\right),$$
$$s(t) = \mathbf{F}\left(\mathbf{q}/2\right)\cdot\hat{\boldsymbol{\Lambda}}(\Delta t)\cdot\left[\hat{\mathbf{U}}(\mathbf{q})\cdot\hat{\boldsymbol{\Lambda}}(\Delta t)\right]^{N-1}\cdot\mathbf{F}^{\dagger}\left(-\mathbf{q}/2\right), \qquad (10)$$

where $\mathbf{q} = \gamma\mathbf{G}\cdot\Delta t$; the elements of the matrix $\hat{\mathbf{U}}$, the diagonal matrix $\hat{\boldsymbol{\Lambda}}$, and the vectors $\mathbf{F}$, $\boldsymbol{\varphi}$ are

$$F_k(\mathbf{q}) = \frac{1}{V}\int_V d\mathbf{r}\, u_k(\mathbf{r})\exp\left(i\mathbf{q}\,\mathbf{r}\right),$$

$$\varphi_k(\mathbf{r},\mathbf{q}) = \frac{1}{V}u_k(\mathbf{r})\exp\left(i\,\mathbf{q}\,\mathbf{r}\right), \qquad (12)$$

$$U_{kk'} = \frac{1}{V}\int_V d\mathbf{r}\, u_k^*(\mathbf{r})u_{k'}(\mathbf{r})\exp\left(i\mathbf{q}\,\mathbf{r}\right),$$

$$\Lambda_{kk} = \exp\left(-\lambda_k\,\Delta t\right). \qquad (13)$$

For the Stejskal–Tanner pulse sequence, the SE signal is equal to

$$s_{SE}(t) = \hat{\mathbf{T}}\cdot\hat{\mathbf{T}}^{\dagger}, \quad \hat{\mathbf{T}} = \mathbf{F}\left(\mathbf{q}/2\right)\cdot\hat{\boldsymbol{\Lambda}}(\Delta t)\cdot\left[\hat{\mathbf{U}}(\mathbf{q})\cdot\hat{\boldsymbol{\Lambda}}(\Delta t)\right]^{N/2-1}. \qquad (14)$$

By choosing the number N big enough, Eqs. (11)–(14) allow to calculate the signal and magnetization distribution with any prescribed accuracy.

A single-compartment model — Edge Enhancement Effect

In the case of one-dimensional diffusion, in which the spins are distributed between two infinite parallel planes localized at positions $x = 0$ and $x = 2a$, a solution to the diffusion equation with reflecting boundary conditions $\partial P/\partial x|_{x=0} = \partial P/\partial x|_{x=2a} = 0$ is well-known (e.g., [13]) and is given by Eq. (10) with

$$u_k(x) = \eta_k\cos\frac{\pi k x}{2a}, \quad \lambda_k = \frac{D_0\beta_k^2}{a^2}, \quad \beta_k = \frac{\pi k}{2} \qquad (15)$$

where the normalization factors are $\eta_0 = 1$, $\eta_{k\neq 0} = \sqrt{2}$. For the gradient symmetric with respect to the center of the interval,

$$F_k = \eta_k f_k, \qquad U_{kk'} = \frac{\eta_k\,\eta_{k'}}{2}\left[f_{k+k'} + f_{|k-k'|}\right], \qquad (16)$$

$$f_k = \frac{2i\Phi}{\left[(\pi k)^2 - 4\Phi^2\right]}\left[-\exp\left(-i\Phi\right) + (-1)^k\exp\left(i\Phi\right)\right],$$

$$\Phi = Qa = \gamma G a\,\Delta t. \qquad (17)$$

There are two characteristic time parameters in the model, determining the signal behavior: the characteristic diffusion time $t_D \equiv a^2/D_0$, and the dephasing time $t_c \equiv 1/(\gamma G a)$, which defines the time of signal dephasing in the absence of diffusion. If we measure time in the units of one of these characteristic times, for example, t_c, the FID signal dependence on $\tau = t/t_c$ will be governed by the sole dimensionless

$$p = \frac{t_c}{t_D} = \frac{D_0}{\gamma\, G\, a^3}. \qquad (18)$$

Figure 2 illustrates the FID signal dependence on the dimensionless time $\tau = t/t_c$ for different values of the parameter p. Note that for small values of the parameter p (including the static case $p = 0$), the signal oscillates with time, whereas for higher p, its behavior becomes monotonic (the detailed analysis shows that the transition takes place at $p = 0.443$). For $p \sim 1$, the GPA is valid, the signal can be describes by the following expression obtained from Eq. (8):

$$s^{(GPA)}(\tau) = \exp\left[-\frac{2}{p^2}\sum_{k=1}^{\infty}\frac{g(p\beta_{2k-1}^2\tau)}{\beta_{2k-1}^8}\right] \qquad (19)$$

where $g(x) = \exp(-x) + x - 1$.

The first line in Eq. (11) (and the corresponding expression for the SE signal) was used to calculate the magnetization distribution and illustrates the so-called edge enhancement effect (see Fig. 3), where the FID (solid lines) and SE (dashed lines) magnetization distribution for the 1D model is plotted as a function of the dimensionless coordinate $x/(2a)$ for two values of the parameter, $p = 0.005$ (curves *1*) and $p = 1$ (curves *2*) (time is fixed, $\tau = 10$). The curves *1* have pronounced maxima at the boundaries, whereas curves *2* are practically flat.

The physical origin of this effect is that spin diffusion in the vicinity of system boundaries is effectively more restricted than that away from the boundaries. The edge enhancement effect takes place when two conditions are satisfied: 1) a characteristic diffusion distance $x_0 \sim (D_0 t)^{1/2}$ that a spin travels over time t is much smaller than a system size a, $x_0 << a$, in other words, $t << t_D$; 2) the field gradient is strong enough to result in a substantial phase difference over x_0: $\gamma G x_0 t \gg 1$, i.e., $t \gg (t_c^2 t_D)^{1/3}$ (note that the combination in the right-hand side of the latter inequality is independent from the system size a). In dimensionless variables, these conditions are $p^{-1/3} \ll \tau \ll p^{-1}$. Obviously, this double-

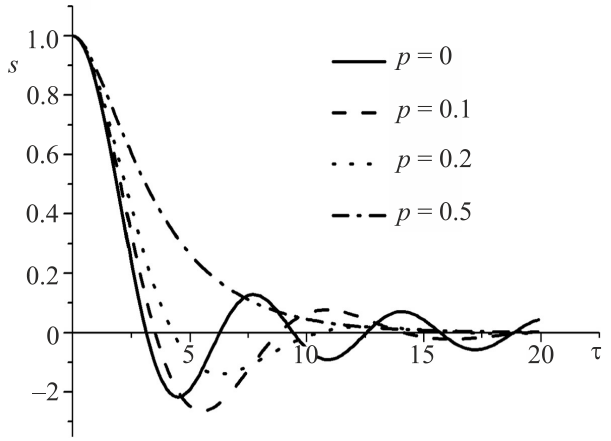

Fig. 2. The FID signal dependence in the 1D model on the dimensionless time $\tau = t/t_c$ for different values of the parameter p.

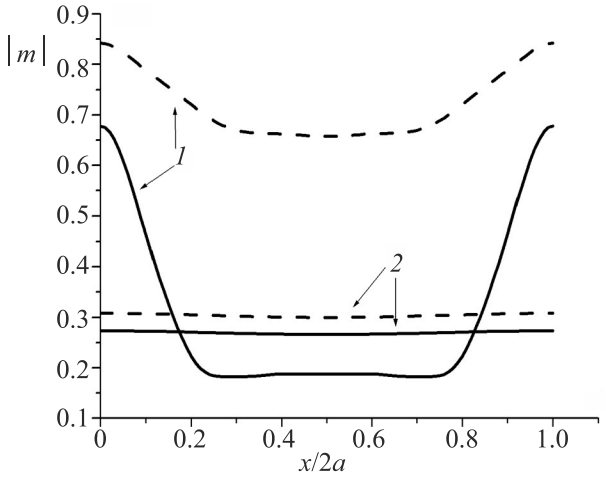

Fig. 3. The magnitude of the FID (solid lines) and SE (dashed lines) signal density $|m|$ as a function of the dimensionless coordinate $x/(2a)$ for the fixed time $\tau = t/t_c = 10$ and $p = 0.005$ (curves *1*) and $p = 1$ (curves *2*). The edge enhancement is pronounced in curves *1* ($t = 0.05 t_D$), and is practically absent in curves *2* ($t = t_D$).

inequality can hold only for $p << 1$. In the case $t \geq t_D$, diffusion "stirs" all spins and the signal density becomes practically homogeneous at time t.

Short time regime

As already mentioned above, the MPA requires the knowledge of the diffusion propagator, i.e., a solution of the diffusion equation with system-specified boundary conditions. Unfortunately, this is possible only in some simple geometries: segment, sphere, cube, etc.). Generally, such a solution is not available in an analytical form. Here we discuss another approach which is applicable for an arbitrary geometry in the short-time regime, when the diffusion time t is much smaller than the characteristic diffusion time t_D,

$$t << t_D = \frac{1}{D_0\left(\sigma/d\right)^2}, \qquad (20)$$

where $\sigma = (A/V)$ is the surface-to-volume ratio, and d is the system's dimensionality.

In this regime, an *effective* time-dependent diffusion coefficient $D(t)$ relating the mean square displacement of a diffusing particle $\langle(\delta\mathbf{r})^2\rangle_t$ and diffusion time t as $\langle(\delta\mathbf{r})^2\rangle_t = 2dD(t)\cdot t$, can be presented in the following universal form [14]:

$$D(t) = D_0\left[1 - c_0\frac{\sigma}{d}(D_0 t)^{1/2}\right], \quad c_0 = \frac{4}{3\sqrt{\pi}}. \qquad (21)$$

Combining Eqs. (7), (8) and (21), the signal can be presented in the monoexponential form of Eq. (9) with the ADC $\tilde{D}_G(t)$

$$\tilde{D}_G(t) = D_0\left[1 - c_G\frac{\sigma}{d}(D_0 t)^{1/2}\right], \quad c_G = c_0\frac{I_{3/2}^{(G)}(t)}{I_1^{(G)}(t)},$$

$$I_n^{(G)}(t) = \int_0^t d\tau_1 \int_0^{\tau_1} d\tau_2\, G(\tau_1)G(\tau_2)(\tau_1 - \tau_2)^n, \tag{22}$$

where the subscript index "G" is used to emphasize that the quantity $\tilde{D}_G(t)$ and the coefficient c_G depend, in general, not only on diffusion time t but on a time-course of the diffusion sensitizing gradient as well.

For the Stejskal–Tanner pulse sequence with the time parameters Δ and δ [15]:

$$c_G(\Delta,\delta) = \frac{16}{35\sqrt{\pi}}\frac{\left[(\Delta+\delta)^{7/2} + (\Delta-\delta)^{7/2} - 2\Delta^{7/2} - 2\delta^{7/2}\right]}{\delta^2\left(\Delta - \delta/3\right)(\Delta+\delta)^{1/2}}. \tag{23}$$

If $\delta << \Delta$ (narrow pulse approximation, diffusion during the gradient pulses is ignored), $c_G = c_0$

In [16,17], Eqs. (21), (22) were applied to the oscillating gradient sequence. The latter is extensively used for studying short-length scales inhomogeneities in porous media and biological systems. For the oscillating gradient $G(t) = G_0 \cdot \cos(\omega t - \varphi)$ with N total periods of oscillations, the ADC $\tilde{D}_G$ as a function of frequency ω and a number of oscillations N can be presented as

$$\tilde{D}_G(t = 2\pi N/\omega) = D_0\left(1 - \frac{c'}{\Omega^{1/2}}\right), \quad c' = c_G\cdot(2\pi N)^{1/2}, \tag{24}$$

$$c'(\varphi, N) =$$

$$= \frac{32\pi N^{3/2}\sin^2\varphi + 12\pi N\cdot C(2N^{1/2}) + 3(3 + 4\sin^2\varphi)\cdot S(2N^{1/2})}{6\sqrt{2}\,\pi N(1 + 2\sin^2\varphi)} \tag{25}$$

where $\Omega = \omega t_D$; $C(x)$ and $S(x)$ are the Fresnel functions.

For any $\varphi \neq 0$ (including *sin*-type gradient), the coefficient $c'(\varphi, N)$ monotonically increases at large N, whereas for $\varphi = 0$ (*cos*-type gradient), the coefficient $c'(0, N)$ monotonically decreases with N increases and tends to a finite value $1/\sqrt{2}$:

$$c'_{\cos}(N) \equiv c'(\varphi = 0, N) = \frac{1}{\sqrt{2}}\left(1 - \frac{1}{\pi^2 N^{3/2}}\right), \quad N >> 1,$$

$$c'(\varphi \neq 0, N) = \frac{8\sqrt{2}\sin^2\varphi}{3(1 + 2\sin^2\varphi)}N^{1/2}, \quad N >> 1. \tag{26}$$

The divergence of the coefficient $c'(\varphi \neq 0, N)$ at large N imposes a restriction on the oscillation number N: $c'(\varphi \neq 0, N)/\Omega^{1/2} << 1$, that is equivalent to the requirement of the short-time approximation, $t << t_D$. Interestingly, this requirement can be lifted for the *cos*-type gradient because $c'_{\cos} \sim 1$ for any N. The detailed analysis of this issue can be found in [17].

Concluding remarks

In this paper, we have discussed several theoretical approaches developed for describing diffusion-attenuated MR signals in biological structures. As such structures are extremely complex with great variability of structural units (cells), it is not possible to propose an exact microscopically-based model which would capture all microstructural properties of biological tissues. Thus, different approaches are developed to address different aspects of the tissue complexity. For example, the multi-propagator approach can be used for theoretical analysis of diffusion-attenuated MR signal in simplified geometries (e.g. spherical cells). On the other hand, the Gaussian phase approximation is based on the statistical properties of water molecules diffusing in a complex cellular environment thus relating theoretical parameters to tissue microstructure.

Acknowledgement

This work was supported by US NIH grant R01AG054513.

1. E.O. Stejskal and J.E. Tanner, *J. Chem. Phys*. **42**, 288 (1965).
2. H.C. Torrey, *Phys. Rev*. **104**, 563 (1956).
3. S.D. Stoller, W. Happer, and F.J. Dyson, *Phys. Rev. A* **44**, 7459 (1991).
4. R.F. Karlicek, Jr. and I.J. Lowe, *J. Magn. Reson*. **37**, 75 (1980).
5. D.C. Douglass and D.W. McCall, *J. Phys. Chem*. **62**, 1102 (1958).
6. C.H. Neuman, *J. Chem. Phys*. **60**, 4508 (1973).
7. P.T. Callaghan, *Principles of Nuclear Magnetic Resonance Microscopy*, Claredon Press, Oxford (1991).
8. L.Z. Wang, A. Caprihan, and E. Fukushima, *J. Magn. Reson., Ser. A* **117**, 209 (1995).
9. J. Stepisnik, *Physica B* **270**, 110 (1999).
10. A.L. Sukstanskii and D.A. Yablonskiy, *J. Magn. Reson*. **157**, 92 (2002).
11. A. Caprihan, L.Z. Wang, and E. Fukushima, *J. Magn. Reson., Ser. A* **118**, 94 (1995).
12. P.T. Callaghan, *J. Magn. Reson*. **129**, 74 (1997).
13. H.S. Carslaw and J.C. Jaeger, *Conduction of Heat in Solids*, Claredon Press, Oxford (1959).
14. P.P. Mitra, P.N. Sen, and L.M. Schwartz, *Phys. Rev. B* 47, 8565 (1993).
15. L.J. Zielinski and M.D. Hurlimann, *J. Magn. Reson*. **171**, 107 (2004).
16. A.L. Sukstanskii, *J. Magn. Reson*. **234**, 135 (2013).
17. A.L. Sukstanskii and J.J.H. Ackerman, *J. Magn. Reson*. **296**, 165 (2018).

Теоретичні моделі магнітно-резонансного сигналу у біологічних тканинах

Alexander L. Sukstanskii, Dmitriy A. Yablonskiy

Дифузійна магнітно-резонансна томографія (МРТ) відіграє дуже важливу роль у вивченні клітинної структури біологічних тканин та їх функціонування як у нормальному стані, так і при захворюваннях. Коректна інтерпретація експериментальних даних вимагає розробки теоретичних моделей, які пов'язують дифузний МРТ сигнал з характерними особливостями мікроструктури тканини на клітинному рівні. У статті представлено деякі теоретичні підходи щодо опису магнітно-резонансних сигналів. Цей діапазон підходів змінюється від моделей, що засновані на розгляді статистичних властивостей молекул води, які дифундують у тканинно-клітинному середовищі, та до моделей, які дозволяють проводити точний аналітичний розрахунок магнітно-резонансного сигналу у конкретному однокамерному середовищі. Такий теоретичний аналіз дає важливу інформацію про механізми, що сприяють формуванню дифузного магнітно-резонансного сигналу та його зв'язку з клітинною структурою біологічної тканини.

Ключові слова: магнітний резонанс, гауссівське фазове наближення, метод множинного пропагатора.

.